

Extended results for paper Dynamic line-switching in transmission system operation amidst wildfire-prone weather under decision-dependent uncertainty

Juan-Alberto Estrada-Garcia, Ruiwei Jiang

Department of Industrial and Operations Engineering, University of Michigan, Ann Arbor, MI, {juanest@umich.edu, ruiwei@umich.edu}

Alexandre Moreira

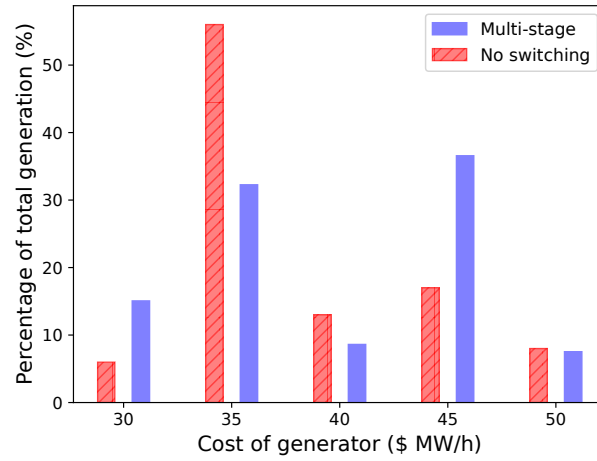
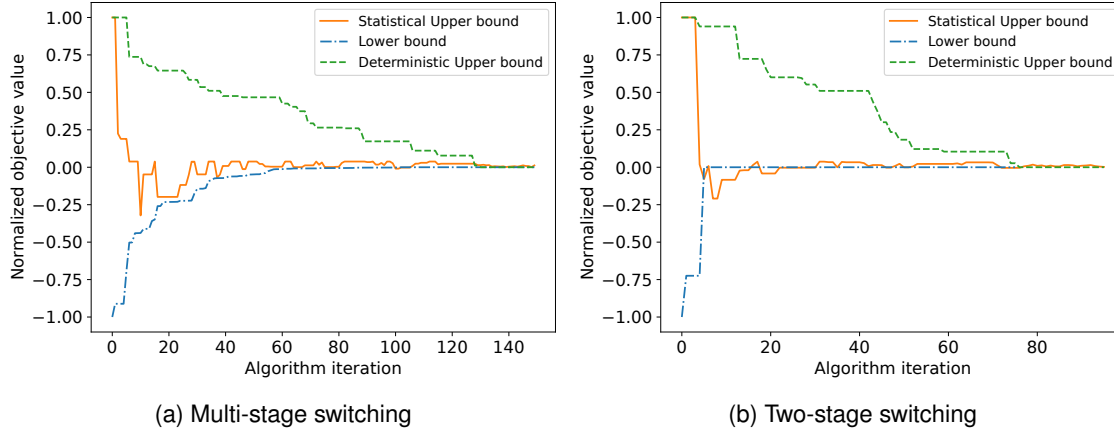
Lawrence Berkeley National Laboratory, Berkeley, CA, amoreira@lbl.gov

Authors are encouraged to submit new papers to INFORMS journals by means of a style file template, which includes the journal title. However, use of a template does not certify that the paper has been accepted for publication in the named journal. INFORMS journal templates are for the exclusive purpose of submitting to an INFORMS journal and are not intended to be a true representation of the article's final published form. Use of this template to distribute papers in print or online or to submit papers to another non-INFORM publication is prohibited.

Abstract. During dry and windy seasons, environmental conditions significantly increase the risk of wildfires, exposing power grids to disruptions caused by transmission line failures. Wildfire propagation exacerbates grid vulnerability, potentially leading to prolonged power outages. To address this challenge, we propose a multi-stage optimization model that dynamically adjusts transmission grid topology in response to wildfire propagation, aiming to develop an optimal response policy. By accounting for decision-dependent uncertainty, where line survival probabilities depend on usage, we employ distributionally robust optimization to model uncertainty in line survival distributions. We adapt the stochastic nested decomposition algorithm and derive a deterministic upper bound for its finite convergence. To enhance computational efficiency, we exploit the concavity of the Lagrangian dual problem and strengthen Lagrangian cuts generated in early iterations. Using realistic data from the California transmission grid, we demonstrate the superior performance of the dynamic response policies against two-stage alternatives through a comprehensive case study. In addition, we construct easy-to-implement policies that significantly reduce computational burden while maintaining good performance in real-time deployment.

1. Value of dynamic line-switching

We extended our analysis of the differences between MS and NS decisions. We display the distribution of power generation of MS and NS among generators with various costs in Fig. 1, which confirms that MS indeed resort to more expensive generators. This suggests that corrective line switching limited the access to cheaper generators and had to use alternative (more expensive) generators.

Figure 1 Distribution of power generation among generators with various costs**Figure 2** Convergence of switching approaches

2. Computational studies

Table 1 presents the computational performance of the SND Algorithm we propose as a function of the planning horizon T (hours), the number of leaf nodes $|\mathcal{S}_T|$, and the value of β . Table 1 suggests that the runtime of the SND algorithm is more sensitive to the size of the scenario tree than to the length of planning horizon or the value of the DDU parameter β in the ambiguity set.

In Figure 2, we show the convergence curves for the dynamic SND algorithm, as well as for the two-stage setup, where we observe a faster convergence of the lower bound and upper bounds.

3. Sensitivity studies

We extend our analysis of the solutions obtained through the SND algorithm we propose and report the operational cost, load shedding cost, and total cost under different β and γ values in Table 2. The insights remain the same as with the $\beta/\bar{\beta} = 1, \gamma/\bar{\gamma} = 1$ case.

Table 1 Summary of computational performance

T	$ S_T $	$\beta/\bar{\beta}$	Multi-stage		Two-stage	
			Runtime (s)	Gap (%)	Runtime (s)	Gap (%)
6	50	0.7	570	0.05	230	0.03
6	100	0.7	1132	0.11	483	0.10
6	150	0.7	2056	0.13	881	0.09
6	50	1.0	630	0.07	235	0.04
6	100	1.0	1302	0.10	490	0.12
6	150	1.0	2360	0.14	932	0.14
6	50	1.3	650	0.06	270	0.05
6	100	1.3	1320	0.11	680	0.13
6	150	1.3	2356	0.16	1142	0.19
12	50	0.7	880	0.07	485	0.09
12	100	0.7	1892	0.17	994	0.13
12	150	0.7	3885	0.23	2253	0.16
12	50	1.0	934	0.09	520	0.09
12	100	1.0	2009	0.19	1040	0.15
12	150	1.0	3950	0.26	2102	0.14
12	50	1.3	1053	0.11	583	0.09
12	100	1.3	2241	0.23	1245	0.17
12	150	1.3	4198	0.32	2305	0.21
24	50	0.7	1220	0.06	842	0.06
24	100	0.7	2850	0.21	1540	0.17
24	150	0.7	6302	0.26	4301	0.19
24	50	1.0	1480	0.09	850	0.07
24	100	1.0	3104	0.24	1604	0.20
24	150	1.0	6821	0.33	4382	0.23
24	50	1.3	1660	0.12	920	0.13
24	100	1.3	3462	0.33	1820	0.27
24	150	1.3	7407	0.47	4431	0.35

Table 3 compares MS, TS, and NS in operational cost, load shedding cost, and the total cost (Obj.) with different values of parameters β and γ .

4. Out-of-sample testing

We first report the performance of the dynamic policy in Figure 3. We observe that this policy produces similar load losses in training and out-of-sample trees (average across 10 replications). Even in the stress-test tree, the dynamic policy incurs only minor increase in load loss. This demonstrates the robustness of the proposed model and the dynamic policy.

We compare the performance of the three policies in Figures 4–5, which report the performance gap across 10 replications. From these figures, we observe that the dynamic policy consistently outperform the topology and mapping policies in load loss. On the flip side, the dynamic policy achieves this by incurring a higher operational cost.

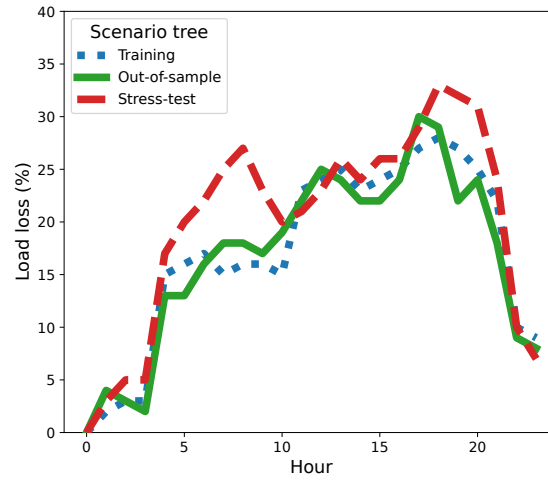
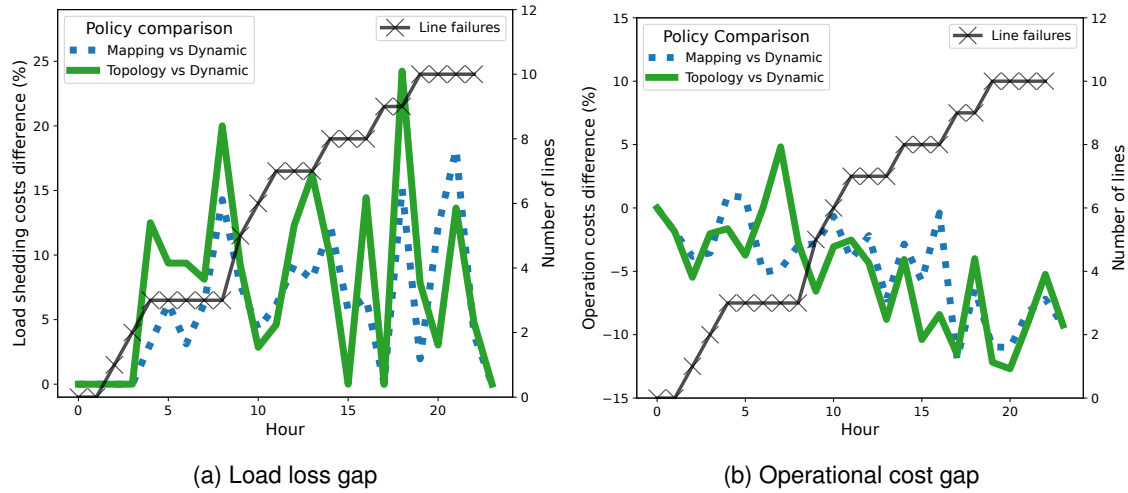
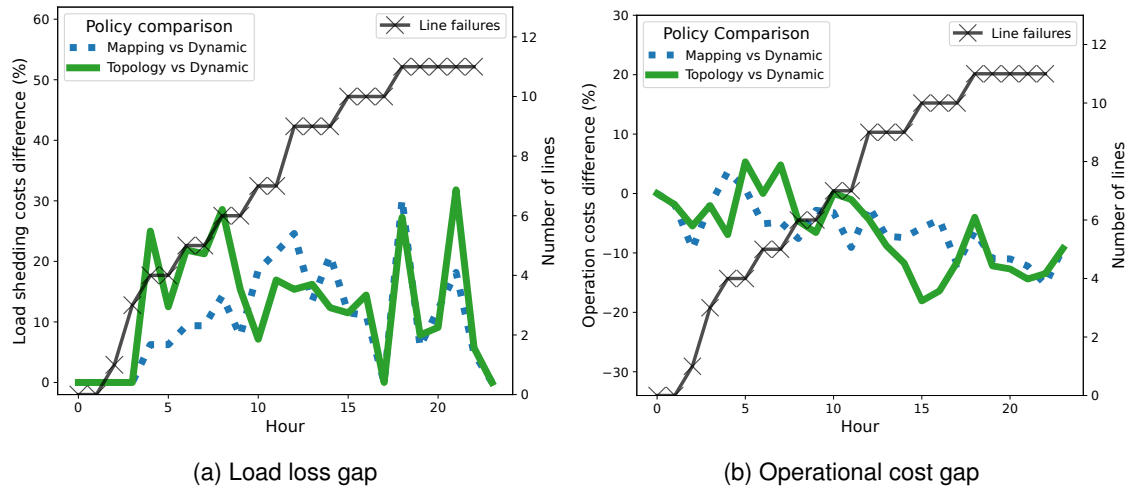
Figure 3 Performance of the dynamic policy in different scenario trees**Figure 4** Performance of the dynamic, topology, and mapping policies in out-of-sample trees**Figure 5** Performance of the dynamic, topology, and mapping policies in stress-test trees

Table 2 Sensitivity analysis for costs of the MS approach

$\beta/\bar{\beta}$	$\gamma/\bar{\gamma}$	Obj. (\$)	Operation (\$)	Load shedding (\$)
0.6	0.6	399890	136128	263762
0.6	0.8	410587	141848	268739
0.6	1.0	461576	150536	311040
0.6	1.2	465577	152048	313529
0.6	1.4	501557	158168	343389
0.8	0.6	471540	160500	311040
0.8	0.8	510948	170048	340900
0.8	1.0	518682	167828	350854
0.8	1.2	529870	174040	355830
0.8	1.4	554806	171604	383202
1.0	0.6	575228	174608	400620
1.0	0.8	591953	181380	410573
1.0	1.0	648512	185684	462828
1.0	1.2	678740	186052	492688
1.0	1.4	691737	191584	500153
1.2	0.6	674233	203940	470293
1.2	0.8	690191	204968	485223
1.2	1.0	746397	211408	534989
1.2	1.2	776852	216980	559872
1.2	1.4	791366	216564	574802
1.4	0.6	832379	222740	609639
1.4	0.8	846972	227380	619592
1.4	1	901367	227032	674335
1.4	1.2	901299	231940	669359
1.4	1.4	918472	234184	684288

We note that the mapping policy shows a better performance, as compared to the topology policy, given its more flexible decision-making. We also note that the dynamic policy has a larger operational cost as compared to the mapping policy and the topology policy, which has the least operational cost. Next, we compare the detailed generation mix of the three policies in Figure 6 under different scenario trees.

We observe a trade off between generator cost and their maximum capacities and the reliability of their associated transmission lines. We note that for the stress test, more expensive generators are employed to improve the reliability of the power delivery. In Figures 5 and 4, we present the gaps between the Mapping and the Topology policies with respect to the dynamic policies, where all of these policies are generated from the scenario tree optimal solutions.

Table 3 Comparison among various approaches with different parameter settings

$\beta/\bar{\beta}$	$\gamma/\bar{\gamma}$	Two-stage vs Multi-stage (%)			No-switching vs Multi-stage (%)		
		Obj.	Operation	Load shedding	Obj.	Operation	Load shedding
0.6	0.6	0.69	-0.06	1.08	23.48	-20.80	46.34
0.6	0.8	9.84	-13.95	22.41	24.98	-23.03	50.32
0.6	1.0	7.10	-21.84	21.11	23.76	-31.93	50.72
0.6	1.2	22.69	-6.32	36.77	21.59	-29.00	46.13
0.6	1.4	9.68	-5.66	16.75	19.20	-24.07	39.14
<hr/>							
0.8	0.6	24.6	-17.79	46.48	32.65	-28.10	64.00
0.8	0.8	16.19	-11.89	30.19	48.28	35.28	54.77
0.8	1.0	12.19	-15.87	25.62	26.55	-29.32	53.27
0.8	1.2	14.75	-11.07	27.37	25.12	-25.12	49.69
0.8	1.4	12.17	-0.31	17.76	28.78	-12.96	47.48
<hr/>							
1.0	0.6	9.46	-14.99	20.12	36.38	-9.98	56.58
1.0	0.8	17.97	-13.01	31.66	36.86	-11.44	58.19
1.0	1.0	15.83	-9.54	26.01	30.13	-11.73	46.92
1.0	1.2	17.35	-10.73	27.95	39.10	0.76	53.58
1.0	1.4	25.08	-6.01	36.99	34.52	-2.84	48.83
<hr/>							
1.2	0.6	19.31	-1.10	28.17	29.77	-9.03	46.60
1.2	0.8	20.06	-2.88	29.74	28.45	-6.2	43.09
1.2	1.0	15.01	-2.45	21.91	23.46	-2.16	33.58
1.2	1.2	17.55	-4.89	26.25	24.51	-4.42	35.72
1.2	1.4	19.22	-3.45	27.76	24.70	-5.46	36.07
<hr/>							
1.4	0.6	25.42	-2.64	35.67	32.64	-12.25	49.04
1.4	0.8	30.76	-2.58	42.99	34.20	-13.95	51.87
1.4	1.0	26.40	-1.51	35.8	32.59	-5.60	45.45
1.4	1.2	28.75	-0.22	38.78	35.43	-5.08	49.46
1.4	1.4	28.72	-0.03	38.56	35.49	-3.40	48.80

Figure 6 Generation mix of the dynamic, topology, and mapping policies